Int. J. Heat Mass Transfer. Vol. 16, pp. 1267–1288. Pergamon Press 1973. Printed in Great Britain

EFFECTS OF BUOYANCY AND OF ACCELERATION OWING TO THERMAL EXPANSION ON FORCED TURBULENT CONVECTION IN VERTICAL CIRCULAR TUBES—CRITERIA OF THE EFFECTS, VELOCITY AND TEMPERATURE PROFILES, AND REVERSE TRANSITION FROM TURBULENT TO LAMINAR FLOW

HIROAKI TANAKA, AYAO TSUGE, MASARU HIRATA and NIICHI NISHIWAKI
Department of Mechanical Engineering, Faculty of Engineering, University of Tokyo, Bunkyo-ku, Tokyo 113, Japan

(*Received* 25 *August* 1972)

Abstract—In this paper, turbulent heat and momentum transfer for a fluid forced through a vertical tube is considered. First, the authors study a shearing-stress distribution in a tube, by taking the buoyancy force and also the inertia force due to acceleration into consideration. It is proved that the effects of both forces operate quite similarly and result in a very rapid decrease of the shearing stress near the wall. By considering how the velocity profile depends upon the shearing-stress gradient at the wall, the authors deduce the criteria for the prominent effects of buoyancy and acceleration. Second, by assuming that the turbulent boundary layer is constructed by the superposition of the locally developed layers, the authors propose an approximate theory to calculate velocity and temperature profiles under the large effects of buoyancy and acceleration. Thirdly, based on the above theory, a criterion of the reverse transition from turbulent to laminar flow is proposed.

NOMENCLATURE

A, conversion factor of heat for work;
c_p, specific heat at constant pressure;
d, tube diameter;
f, friction coefficient $= \dfrac{\tau_w}{(\gamma_f/2g)u_m^2}$;
G, mass velocity;
Gr, Grashof number $= \dfrac{g[(|\gamma_m - \gamma_f|)/\gamma_f]d^3}{\nu_f^2}$;
Gr_a, Grashof number for acceleration $= \dfrac{u_m(\mathrm{d}u_m/\mathrm{d}x)(\gamma_m/\gamma_f)d^3}{\nu_f^2}$;
g, acceleration of gravity;
h, heat-transfer coefficient;
I, total enthalpy flow rate;
i, enthalpy;
K, dimensionless acceleration parameter $= (\nu/u_m^2)(\mathrm{d}u_m/\mathrm{d}x)$;
l, tube length;
M, Mach number;
Nu, Nusselt number $= hd/\lambda_f$;
Pr, Prandtl number $= \nu/\kappa$;
Pr_f, Prandtl number at $T_f = (T_m + T_w)/2$;
Pr_t, turbulent Prandtl number $= \varepsilon_m/\varepsilon_t$;
p, pressure;
q, heat flux;
R, tube radius; gas constant;
Re, Reynolds number $= u_m d/\nu_f$;
Re^*, a kind of Reynolds number $= y^*_{y=R}$;

S_{ao}, S_{go}, S_a, S_g, quantities having a dimension of shearing stress, defined by equations (4), (5), (8) and (9);
T, absolute temperature;
ΔT, wall to bulk temperature difference $= T_w - T_m = t_w - t_m = \Delta t$;
t, temperature; time;
u, axial velocity;
u^+, u^{++}, u^*, dimensionless velocity parameter, defined by equations (67), (71) and (77);
v, specific volume;
W, mass flow rate;
x, axial distance;
y, distance from wall;
y^+, y^{++}, y^*, dimensionless distance parameter, defined by equations (67), (71) and (75);
$y_{\tau=0}$, value of y at which τ vanishes when extrapolated according to the gradient at the wall.

Greek symbols

γ, specific weight;
Δ_τ, dimensionless shearing-stress gradient, defined by equation (97);
δ_l, laminar-sublayer thickness;
δ_t, thermal boundary-layer thickness;
ε_m, eddy diffusivity for momentum;
ε_t, eddy diffusivity for heat;
κ, thermal diffusivity; ratio of specific heat;
λ, thermal conductivity;
μ, dynamic viscosity;
ν, kinematic viscosity;
τ, shearing stress.

Subscripts

a, refers to acceleration;
av, values averaged over tube length;
f, values at film temperature $T_f = (T_m + T_w)/2$; reference values between $y = 0$ and $y = y$; refers to friction;
g, refers to gravity;
m, refers to bulk fluid condition;
w, refers to wall.

1. INTRODUCTION

THE AUTHORS have been studying forced turbulent convection heat transfer to supercritical fluids flowing in circular tubes in recent years [1, 2]. A supercritical fluid shows very large volume change near its critical temperature, and has considerably small kinematic viscosity. Grashof numbers will thus get very large in experiments of heat transfer to supercritical fluids. There arises a question how large Reynolds numbers have to be produced in an experiment in order to make the influence of buoyancy force ineffective. Many literatures [3–8] are available concerning combined free and forced flow in vertical circular tubes. Most of them, however, deal with the laminar flow region where usual cases fall, and only a few deal with the turbulent flow region. Moreover, the above mentioned problem of distinction between forced and free turbulent convection regimes is discussed only by Eckert *et al.* [3, 6].

Further, in regard to the heat transfer to supercritical fluids in tubes, fluid flow may be considerably accelerated owing to its thermal expansion, especially when heated strongly. There arises another question how the inertia force due to acceleration affects the heat-transfer condition. Other than the case of heat transfer to supercritical fluids, several experiments [9–15] have been performed on turbulent heat and momentum transfer for gases in circular tubes at very high wall to bulk temperature ratios, in connection with gas-cooled nuclear reactors and rocket propulsion systems. With respect to these experiments, McEligot *et al.* [16] recently discussed the effect of inertia force on the momentum balance in turbulent boundary layer.

In the following section, the authors will study a shearing-stress distribution in a tube, by taking the buoyancy force and also the inertia

force due to acceleration into consideration. It will be proved that both forces yield a quite similar effect and result in a very rapid decrease of shearing stress near the wall. In Section 3, by considering how the velocity profile depends upon the shearing-stress gradient near the wall, criteria for the predominant effects of buoyancy and acceleration will be deduced. In Section 4, by assuming that the turbulent boundary layer is constructed by the superposition of the locally developed layers, an approximate theory to calculate velocity and temperature profiles under the large effects of buoyancy and acceleration will be proposed. Based on this approximate theory, a reverse transition from turbulent to laminar flow, which has attracted increasing interest in recent years, will be discussed in the last part of Section 4.

2. SHEARING-STRESS DISTRIBUTIONS IN TUBES

Heat transfer for a fluid flowing in a vertically placed circular tube of radius R is now considered. The momentum equation will be derived for the annular section between radii R and $R-y$ (y indicates the distance from the wall surface). In this place, regarding the axial momentum change due to acceleration (deceleration, in case of cooling), the condition of 'quasi-developed' flow may be intuitively assumed. Namely, the velocity profile may be accelerated in a uniform proportion; more strictly, $(1/u)(\mathrm{D}u/\mathrm{D}x) \doteqdot \text{const.}(y) = (1/u_m)(\mathrm{d}u_m/\mathrm{d}x)$ (where $\mathrm{D}/\mathrm{D}x$ indicates the derivative along the streamline). The axial momentum change term is then given as

$$\frac{1}{g}\int_0^y \gamma \frac{\mathrm{D}u}{\mathrm{D}t} 2\pi(R-\eta)\,\mathrm{d}\eta = \frac{1}{g}\int_0^y \gamma u \frac{\mathrm{D}u}{\mathrm{D}x} 2\pi(R-\eta)\,\mathrm{d}\eta \doteqdot \frac{1}{g}\frac{1}{u_m}\frac{\mathrm{d}u_m}{\mathrm{d}x}\int_0^y \gamma u^2 2\pi(R-\eta)\,\mathrm{d}\eta. \quad (1)$$

The momentum equation is expressed by

$$\frac{1}{g}\frac{1}{u_m}\frac{\mathrm{d}u_m}{\mathrm{d}x}\int_0^y \gamma u^2 2\pi(R-\eta)\,\mathrm{d}\eta = -\pi\{R^2-(R-y)^2\}\frac{\mathrm{d}p}{\mathrm{d}x} \mp \int_0^y \gamma 2\pi(R-\eta)\,\mathrm{d}\eta - 2\pi R\tau_w + 2\pi(R-y)\tau \quad (2)$$

where for the sign of the second term on the right-hand side we use either the $-$ or the $+$ sign according as the flow direction is upward or downward. By setting $y = R$ in equation (2), we obtain the momentum equation for the whole tube, which determines the pressure gradient $\mathrm{d}p/\mathrm{d}x$ as

$$-\pi R^2 \frac{\mathrm{d}p}{\mathrm{d}x} = \frac{1}{g}\frac{1}{u_m}\frac{\mathrm{d}u_m}{\mathrm{d}x}\int_0^R \gamma u^2 2\pi(R-\eta)\,\mathrm{d}\eta \pm \int_0^R \gamma 2\pi(R-\eta)\,\mathrm{d}\eta + 2\pi R\tau_w. \quad (3)$$

Obviously, the pressure drop consists of three terms, which are caused, in turn, by the acceleration, the gravity and the wall friction. For brevity, we write the first and the second terms on the right-hand side of equation (3) as

$$2\pi R S_{ao} \equiv \frac{1}{g}\frac{1}{u_m}\frac{\mathrm{d}u_m}{\mathrm{d}x}\int_0^R \gamma u^2 2\pi(R-\eta)\,\mathrm{d}\eta, \quad (4)$$

$$2\pi R S_{go} \equiv \int_0^R \gamma 2\pi(R-\eta)\,\mathrm{d}\eta \quad (5)$$

where S_{ao} and S_{go} denote the equivalent shearing stresses at the wall that might be assigned if the pressure drops due to acceleration and gravity were attributed to the wall friction. Equations (4) and (5) are evaluated approximately as

$$2\pi R S_{ao} \simeq \pi \frac{\gamma_m}{g} u_m \frac{\mathrm{d}u_m}{\mathrm{d}x} R^2,$$

$$\text{i.e. } S_{ao} \simeq \frac{1}{2}\frac{\gamma_m}{g} u_m \frac{\mathrm{d}u_m}{\mathrm{d}x} R, \quad (6)$$

$$2\pi R S_{go} \simeq \pi \gamma_m R^2, \qquad \text{i.e. } S_{go} \simeq \tfrac{1}{2}\gamma_m R. \quad (7)$$

Similarly, the acceleration and the gravity terms in equation (2) may be written as

$$2\pi RS_a \equiv \frac{1}{g}\frac{1}{u_m}\frac{\mathrm{d}u_m}{\mathrm{d}x}\int_0^y \gamma u^2 2\pi(R-\eta)\,\mathrm{d}\eta, \quad (8)$$

$$2\pi RS_g \equiv \int_0^y \gamma 2\pi(R-\eta)\,\mathrm{d}\eta \quad (9)$$

which are evaluated approximately as

$$2\pi RS_a \simeq \pi\frac{1}{g}\frac{1}{u_m}\frac{\mathrm{d}u_m}{\mathrm{d}x}\gamma_f u_f^2\{R^2-(R-y)^2\}, \quad (10)$$

$$2\pi RS_g \simeq \pi\gamma_f\{R^2-(R-y)^2\} \quad (11)$$

where the subscript f denotes the reference values between $y=0$ and $y=y$. By substituting for $\mathrm{d}p/\mathrm{d}x$ from equation (3) into equation (2) and by using equations (4), (5), (8) and (9), the shearing stress τ at y is determined as

$$\tau = \tau_a + \tau_g + \tau_f \equiv \left\{-\left(\frac{R}{R-y}-\frac{R-y}{R}\right)S_{ao} + \frac{R}{R-y}S_a\right\} \pm \left\{-\left(\frac{R}{R-y}-\frac{R-y}{R}\right)S_{go} + \frac{R}{R-y}S_g\right\} + \frac{R-y}{R}\tau_w \quad (12)$$

where τ_a, τ_g and τ_f represent the components which originate from the acceleration, the gravity and the wall friction respectively.

We now inquire into the state of τ near the wall. From equations (6), (7), (10) and (11),

$$\frac{S_a}{S_{ao}} \doteqdot \frac{u_f^2\gamma_f}{u_m^2\gamma_m}\left\{1-\frac{(R-y)^2}{R^2}\right\}, \qquad \frac{S_g}{S_{go}} \doteqdot \frac{\gamma_f}{\gamma_m}\left\{1-\frac{(R-y)^2}{R^2}\right\}. \quad (13)$$

By substituting these into equation (12),

$$\tau = \tau_a + \tau_g + \tau_f \equiv -\left(1-\frac{u_f^2}{u_m^2}\frac{\gamma_f}{\gamma_m}\right)\left(\frac{R}{R-y}-\frac{R-y}{R}\right)S_{ao} \mp \left(1-\frac{\gamma_f}{\gamma_m}\right)\left(\frac{R}{R-y}-\frac{R-y}{R}\right)S_{go} + \frac{R-y}{R}\tau_w. \quad (14)$$

Very near the wall, $(u_f^2/u_m^2) \ll 1$. Therefore,

$$\tau = \tau_a + \tau_g + \tau_f \equiv -2\frac{y}{R}S_{ao} \mp 2\left(1-\frac{\gamma_f}{\gamma_m}\right)\frac{y}{R}S_{go} + \left(1-\frac{y}{R}\right)\tau_w = \tau_w - \left\{2S_{ao} \pm 2\left(1-\frac{\gamma_f}{\gamma_m}\right)S_{go} + \tau_w\right\}\frac{y}{R}. \quad (15)$$

It is noticeable that τ decreases near the wall according to the gradient

$$-\left\{2S_{ao} \pm 2\left(1-\frac{\gamma_f}{\gamma_m}\right)S_{go} + \tau_w\right\},$$

when the distance from the wall is normalized as y/R. On the other hand, the state of τ near the tube centre is easily verified to be in proportion to radius r, by deriving the momentum equation about the volume inside the radius r, which is quite similar to equation (3). As a whole, the distribution of τ will be such as illustrated in Figs. 7 and 9.

3. CRITERIA FOR THE EFFECTS OF BUOYANCY AND ACCELERATION

3.1 *Basic considerations*

For the present, we assume a state of turbulent convection. At first, we presume a state where the effects of acceleration and gravity might be neglected. Then the distribution of shearing stress τ is linear as usual case, and τ is proportional to r. Here, the variation of fluid properties near the wall should be taken into consideration. The conditions of the turbulent boundary layer near the wall may be virtually determined by the reference properties in the boundary layer and by the velocity just outside the boundary layer. Therefore, various formulas for heat and momentum transfer in the case of constant fluid properties may be applied to that of varying properties as a rough approximation, by setting as follows for Reynolds number, friction coefficient, Prandtl number and Nusselt number respectively:

$$Re = \frac{u_m d}{\nu_f}, \qquad f = \frac{\tau_w}{(\gamma_f/2g)u_m^2},$$
$$Pr_f = \nu_f/\kappa_f, \qquad Nu = hd/\lambda_f \qquad (16)$$

where the subscript f denotes the property values at the reference temperature $t_f = (t_w + t_m)/2$. It will be known that this approximation is based on the theory of turbulent convection in case of varying properties which has been developed by the authors concerning the heat transfer to supercritical fluids [1, 2]. (The theory will be extended in the succeeding chapter.) Formerly, Humble *et al.* [17] measured heat-transfer and friction coefficients for air in tubes at wall to bulk temperature ratios T_w/T_m to 2·5, and concluded that the experimental results could be fairly correlated by Dittus–Boelter's formula and Kármán–Nikuradse's formula by using the dimensionless numbers defined in equations (16). Later, Taylor [9, 11, 12] performed experiments for hydrogen and helium at wall to bulk temperature ratios T_w/T_m up to 8·0, and came up to the conclusion that according as T_w/T_m got high the above method of correlation became unsatisfactory especially as for the friction coefficients. These very deviations have to be attributed to the effect of acceleration, and will become clear in the following. Now we assume the turbulent boundary-layer model consisting of two layers [18], and assume for the thickness δ_l of the laminar sublayer that

$$\delta_l^+ \equiv \frac{\sqrt{(g\tau_w/\gamma_f)}}{\nu_f}\delta_l = 12{\cdot}26.$$

By using Blasius' formula: $4f = 0{\cdot}3164\ Re^{-\frac{1}{4}}$, the wall friction τ_w is estimated as

$$\tau_w = f\frac{\gamma_f}{2g}u_m^2 = \frac{0{\cdot}3164}{8}\left(\frac{u_m d}{\nu_f}\right)^{-\frac{1}{4}}\frac{\gamma_f}{g}u_m^2. \qquad (17)$$

Therefore, the proportion of δ_l to R is

$$\frac{\delta_l}{R} = 12{\cdot}26\frac{\nu_f}{\sqrt{\left(\frac{g\tau_w}{\gamma_f}\right)R}}$$
$$= 12{\cdot}26\frac{\nu_f}{\left\{\frac{0{\cdot}3164}{8}\left(\frac{u_m d}{\nu_f}\right)^{-\frac{1}{4}}u_m^2\frac{d^2}{4}\right\}^{\frac{1}{2}}}$$
$$= 123\left(\frac{u_m d}{\nu_f}\right)^{-\frac{7}{8}}. \qquad (18)$$

The actual shearing-stress distribution under the influences of buoyancy and acceleration is expressed by equation (15). For the sake of brevity, we assume the case of upward heated flow, where all the terms in { } of equation (15) are positive. If we extrapolate the value of τ linearly according to the gradient near the wall, τ may vanish at $y_{\tau=0}$ determined by

$$\frac{y_{\tau=0}}{R} = \frac{\tau_w}{2S_{ao} + 2\left(1 - \frac{\gamma_f}{\gamma_m}\right)S_{go} + \tau_w}$$
$$= \frac{1}{2\frac{S_{ao}}{\tau_w} + 2\left(1 - \frac{\gamma_f}{\gamma_m}\right)\frac{S_{go}}{\tau_w} + 1}. \qquad (19)$$

We presumed at the beginning the state where the effects of acceleration and gravity were neglected. Here we examine whether the velocity profile determined from that assumption (where τ is almost constant near the wall) is consistent with the actual shearing-stress distribution expressed by equation (15). Keeping in mind that the mean velocity (in consequence, the flow rate) is virtually determined by the velocity profile (accordingly, by the shearing-stress distribution) in the laminar sublayer, if $\tau_{y=0} \gg \delta_l$, the wall friction and the velocity profile presumed at the beginning almost agree with the actual ones, although the actual shearing-stress distribution may considerably differ from the presumed one especially at a distance from the wall. On the other hand, if $y_{\tau=0} \leqslant \delta_l$, the velocity profile presumed at the beginning is entirely inconsistent with the actual shearing-stress distribution. By comparing the case where $\tau = \text{const.} = \tau_w$ in the laminar sublayer with the case where τ decreases linearly from the same τ_w at the wall to zero at the border, it will easily be shown that the velocity just outside

the laminar sublayer in the former case is two times as large as that in the latter case, on the assumption that the thickness of the laminar sublayer remains unchanged. Therefore, the actual wall friction may well exceed the presumed one in order that the given flow rate might be forced through. From the above considerations, the criterion for the prominent effects of buoyancy and acceleration is given as

$$y_{\tau=0} \leqslant \delta_l. \tag{20}$$

This is rewritten by using equations (18) and (19) as

$$\frac{1}{2\dfrac{S_{ao}}{\tau_w} + 2\left(1 - \dfrac{\gamma_f}{\gamma_m}\right)\dfrac{S_{go}}{\tau_w} + 1} \leqslant 123\left(\frac{u_m d}{\nu_f}\right)^{-\frac{7}{8}}. \tag{21}$$

When $Re = 5000, 20000$, the right-hand side of equation (21) amounts to $\delta_l/R = \frac{1}{14}, \frac{1}{48}$ respectively. Therefore, when the condition (21) is fulfilled, the unity in the denominator on the left-hand side may be neglected. As a result, the basic condition to discriminate the large effects of buoyancy and acceleration in case of upward heated flow is written as

$$\frac{1}{2\dfrac{S_{a0}}{\tau_w} + 2\left(1 - \dfrac{\gamma_f}{\gamma_m}\right)\dfrac{S_{go}}{\tau_w}} \leqq 123\left(\frac{u_m d}{\nu_f}\right)^{-\frac{7}{8}}. \tag{22}$$

From equations (3)–(5), τ_w is in proportion to the pressure drop Δp_f due to the wall friction, and so are S_{ao} and S_{go} to Δp_a due to the acceleration and to Δp_g due to the gravity respectively. Accordingly, in equation (22),

$$\frac{S_{ao}}{\tau_w} = \frac{\Delta p_a}{\Delta p_f}, \qquad \frac{S_{go}}{\tau_w} = \frac{\Delta p_g}{\Delta p_f}. \tag{23}$$

3.2 *Criteria for the buoyancy effect*

First, we inquire into the simple buoyancy effect. From equation (22),

$$\frac{1}{2\left(1 - \dfrac{\gamma_f}{\gamma_m}\right)\dfrac{S_{go}}{\tau_w}} \leqslant 123\left(\frac{u_m d}{\nu_f}\right)^{-\frac{7}{8}}. \tag{24}$$

From equations (7) and (17),

$$\left(1 - \frac{\gamma_f}{\gamma_m}\right)\frac{S_{go}}{\tau_w} \doteqdot \left(1 - \frac{\gamma_f}{\gamma_m}\right) \frac{\dfrac{\gamma_m d}{4}}{\dfrac{0{\cdot}3164}{8}\left(\dfrac{u_m d}{\nu_f}\right)^{-\frac{1}{4}}\dfrac{\gamma_f u_m^2}{g}}$$

$$= 6{\cdot}32\left(\frac{g\dfrac{\gamma_m - \gamma_f}{\gamma_f} d^3}{\nu_f^2}\right)\left(\frac{u_m d}{\nu_f}\right)^{-\frac{7}{4}} \tag{25}$$

where

$$Gr \equiv \frac{g\dfrac{\gamma_m - \gamma_f}{\gamma_f} d^3}{\nu_f^2} \tag{26}$$

is a Grashof number. Substituting equation (25) into equation (24), we obtain

$$Re^{\frac{21}{8}} \leqslant 1{\cdot}55 \times 10^3\, Gr \tag{27}$$

for the condition to discriminate the large effect of buoyancy in case of upward heated flow.

In the above discussions, we have considered mainly from the standpoint with respect to the momentum boundary layer (otherwise, on the assumption that the thermal boundary layer is thicker than the momentum boundary layer). So Prandtl number does not appear in the resulting equation (27). The proportion of the thickness of the thermal boundary layer to that of the momentum boundary layer is estimated roughly as $\delta_t/\delta_l \simeq Pr^{-0{\cdot}4}$. (Refer to equation (42).) When $Pr > 1$ and $\delta_t < \delta_l$, it seems more reasonable to adopt

$$y_{\tau=0} \leqslant \delta_t (< \delta_l) \tag{28}$$

in place of equation (20). From the definition, $y_{\tau=0}$ merely means the point where τ might vanish by extrapolation according to the gradient of τ at the wall. On the other hand, equation (28) ensures that the extrapolated point $y_{\tau=0}$ exists inside the thermal boundary layer so that the shearing stress may actually decrease to zero near the wall. According to the above considera-

tion, we obtain by multiplying the right-hand side of equation (24) by $Pr_f^{-0.4}$ and rearranging

$$Re^{\frac{7}{8}} \leqslant 1{\cdot}55 \times 10^3\, Gr\, Pr_f^{-0.4} \text{ (for } Pr_f > 1) \quad (29)$$

in place of equation (27).

3.3 *Criteria for the acceleration effect*

Next, we inquire into the simple acceleration effect due to thermal expansion. From equation (22),

$$\frac{1}{2(S_{ao}/\tau_w)} \leqq 123\left(\frac{u_m d}{\nu_f}\right)^{-\frac{7}{8}}. \quad (30)$$

From equations (6) and (17), we obtain in the same way as equation (25) was derived

$$\frac{S_{ao}}{\tau_w} \doteqdot 6{\cdot}32\left(\frac{u_m \dfrac{\mathrm{d}u_m}{\mathrm{d}x}\dfrac{\gamma_m}{\gamma_f} d^3}{\nu_f^2}\right)\left(\frac{u_m d}{\nu_f}\right)^{-\frac{7}{4}}. \quad (31)$$

Since $u_m(\mathrm{d}u_m/\mathrm{d}x)$ is a mean acceleration in x direction,

$$Gr_a \equiv \frac{u_m \dfrac{\mathrm{d}u_m}{\mathrm{d}x}\dfrac{\gamma_m}{\gamma_f} d^3}{\nu_f^2} \quad (32)$$

is a Grashof number representing the acceleration effect. Substituting equation (31) into equation (30), we obtain

$$Re^{\frac{7}{8}} \leqslant 1{\cdot}55 \times 10^3\, Gr_a \quad (33)$$

for the condition to discriminate the large effect of acceleration in case of heated flow. At this juncture, the modification for the case of high Prandtl number introduced in the preceding section is considered to be insignificant in the present case. Because, in equation (14) which represents the shearing stress near the wall, the component τ_g due to gravity has a factor $[1 - (\gamma_f/\gamma_m)]$ and is closely related to the thermal boundary layer. On the other hand, the component τ_a due to acceleration has a factor $[1 - (u_f^2/u_m^2)(\gamma_f/\gamma_m)]$, which was supposed to be near unity in deriving equation (15) from equation (14), by taking account that $u_f^2/u_m^2 \ll 1$ in the momentum boundary layer.

The acceleration factor $u_m(\mathrm{d}u_m/\mathrm{d}x)$ in equation (32) is related to the heat flux q_w as follows. Since the cross-section of the tube and the flow rate are constant, we obtain from the condition of continuity

$$\frac{1}{u_m}\frac{\mathrm{d}u_m}{\mathrm{d}x} = \frac{1}{v_m}\frac{\mathrm{d}v_m}{\mathrm{d}x}. \quad (34)$$

If only the volume change owing to thermal expansion under constant pressure is considered (in the Appendix, we consider the case of high velocity flow where the volume change due to pressure drop plays an important role),

$$\frac{1}{u_m}\frac{\mathrm{d}u_m}{\mathrm{d}x} = \frac{1}{v_m}\left(\frac{\mathrm{d}v}{\mathrm{d}i}\right)_m \frac{\mathrm{d}i_m}{\mathrm{d}x} = \frac{1}{v_m}\left(\frac{\mathrm{d}v}{\mathrm{d}i}\right)_m \frac{\pi d q_w}{\frac{\pi}{4}d^2 u_m \gamma_m} = \left(\frac{\mathrm{d}v}{\mathrm{d}i}\right)_m \frac{4q_w}{\mathrm{d}u_m}. \quad (35)$$

Whence,

$$u_m \frac{\mathrm{d}u_m}{\mathrm{d}x} = \left(\frac{\mathrm{d}v}{\mathrm{d}i}\right)_m \frac{4q_w u_m}{d}. \quad (36)$$

For the particular case of a perfect gas,

$$u_m \frac{\mathrm{d}u_m}{\mathrm{d}x} = \frac{v_m}{c_{p_m} T_m}\frac{4q_w u_m}{d}. \quad (37)$$

Further, by eliminating q_w we can rewrite the condition (33) in terms of the wall to bulk temperature difference $\Delta t = t_w - t_m = T_w - T_m = \Delta T$. Coming back to equation (6) and using equation (36),

$$\frac{S_{ao}}{\tau_w} \doteqdot \frac{\frac{d}{4}\dfrac{\gamma_m}{g} u_m \dfrac{\mathrm{d}u_m}{\mathrm{d}x}}{\tau_w} = \left(\frac{\mathrm{d}v}{\mathrm{d}i}\right)_m \frac{\gamma_m u_m}{g}\frac{q_w}{\tau_w}. \quad (38)$$

For the case of a perfect gas, using equation (37) instead of equation (36),

$$\frac{S_{ao}}{\tau_w} = \frac{u_m}{g c_{p_m} T_m}\frac{q_w}{\tau_w}. \quad (39)$$

From those mentioned about equation (16), the heat-transfer coefficient h may be estimated as follows on the basis of Dittus–Boelter's formula;

$$\frac{hd}{\lambda_f} = 0{\cdot}023 \left(\frac{u_m d}{\nu_f}\right)^{0{\cdot}8} Pr_f^{0{\cdot}4}. \quad (40)$$

Setting $q_w = h\Delta t$ and using equation (17) for τ_w, q_w/τ_w in equations (38) and (39) is calculated as

$$\frac{q_w}{\tau_w} = \frac{0{\cdot}023 \left(\frac{u_m d}{\nu_f}\right)^{0{\cdot}8} Pr_f^{0{\cdot}4} \frac{\lambda_f}{d} \Delta t}{\frac{0{\cdot}3164}{8} \left(\frac{u_m d}{\nu_f}\right)^{-\frac{1}{4}} \frac{\gamma_f}{g} u_m^2}$$

$$= 0{\cdot}581 \left(\frac{u_m d}{\nu_f}\right)^{0{\cdot}05} Pr_f^{-0{\cdot}6} \frac{gc_{p_f}\Delta t}{u_m}. \quad (41)$$

According to Reynolds' analogy, the above equation must be reduced to $q_w/\tau_w = gc_{p_f}\Delta t/u_m$ for $Pr_f = 1$ [19]. Therefore, the numerical coefficient and the exponent of Reynolds number in equation (41) are considered to be attributed to that equations (17) and (40) are empirical correlations. Thus the following equation suffices to estimate the influence of Prandtl number.

$$\frac{q_w}{\tau_w} = Pr_f^{-0{\cdot}6} \frac{gc_{pf}\Delta t}{u_m}. \quad (42)$$

Substituting this into equation (38) and also into equation (39) gives

$$\frac{S_{ao}}{\tau_w} = \left\{\left(\frac{1}{v}\frac{dv}{di}\right)_m c_{p_f}\Delta t\right\} Pr_f^{-0{\cdot}6} \quad (43)$$

for the general case, and

$$\frac{S_{ao}}{\tau_w} = \frac{c_{pf}}{c_{p_m}} \frac{\Delta T}{T_m} Pr_f^{-0{\cdot}6} \quad (44)$$

for the particular case of a perfect gas. By substituting these into equation (30), we obtain as the condition to discriminate the large effect of acceleration in case of heated flow

$$Re^{\frac{1}{8}} Pr_f^{0{\cdot}6} \leqslant 246 \left\{\left(\frac{1}{v}\frac{dv}{di}\right)_m c_{p_f}\Delta t\right\} \quad (45)$$

for the general case, and

$$Re^{\frac{1}{8}} Pr_f^{0{\cdot}6} \leqslant 246 \frac{c_{pf}}{c_{p_m}} \frac{\Delta T}{T_m} \quad (46)$$

for the particular case of a perfect gas. For example, when $c_{p_f} = c_{p_m}$, $Pr_f = 1$ and $Re = 4000$, equation (46) is reduced to $(\Delta T/T_m) \geqslant 5{\cdot}77$, namely, $(T_w/T_m) \geqslant 6{\cdot}77$.

3.4 *Laminar-flow case; distinctions between heated and cooled flows and also between upward and downward flows*

Hitherto this chapter dealt with the case of turbulent flow. The case of laminar flow can be treated more easily, and will be summarized in the following. For upward heated laminar flow, the basic condition to discriminate the large effects of buoyancy and acceleration may be given as

$$y_{\tau=0} \leqslant \frac{R}{N} \quad (47)$$

in place of equation (20) for turbulent flow. The value of N may range between 2·0 and 3·0. In the following calculations, it is assumed that $N = 3{\cdot}0$. By using equation (19), equation (47) is transformed into

$$\frac{S_{ao}}{\tau_w} + \left(1 - \frac{\gamma_f}{\gamma_m}\right)\frac{S_{go}}{\tau_w} \geqslant 1. \quad (48)$$

If the effects of acceleration and gravity were neglected, the wall friction for laminar flow in a tube might be given as

$$\tau_w = \frac{16}{(u_m d/\nu_f)} \frac{\gamma_f}{2g} u_m^2 = 8 \frac{\mu_f u_m}{d}. \quad (49)$$

Therefore, in place of equation (25) for turbulent flow, we obtain

$$\left(1 - \frac{\gamma_f}{\gamma_m}\right)\frac{S_{go}}{\tau_w} = \left(1 - \frac{\gamma_f}{\gamma_m}\right)\frac{(\gamma_m d/4)}{8(\mu_f u_m/d)}$$

$$= \frac{1}{32}\left(\frac{g[(\gamma_m - \gamma_f)/\gamma_f]d^3}{\nu_f^2}\right)\left(\frac{u_m d}{\nu_f}\right)^{-1}. \quad (50)$$

Substituting this into equation (48), we obtain

$$Gr\, Re^{-1} \geqslant 32 \quad (51)$$

for the condition to discriminate the large effect of buoyancy in case of upward heated laminar

flow. At this juncture, we need not introduce the modification for the effect of Prandtl number which was considered in equation (29), because the temperature profile for the fully developed laminar flow is independent of Prandtl number.

Next, in place of equation (31) for turbulent flow,

$$\frac{S_{ao}}{\tau_w} = \frac{1}{32}\left(\frac{u_m(\mathrm{d}u_m/\mathrm{d}x)(\gamma_m/\gamma_f)d^3}{\nu_f^2}\right)\left(\frac{u_m d}{\nu_f}\right)^{-1}. \quad (52)$$

Therefore, we obtain

$$Gr_a Re^{-1} \geqslant 32 \quad (53)$$

for the condition to discriminate the large effect of acceleration in case of heated laminar flow. Although the heat-transfer coefficient for fully developed laminar flow in tubes is slightly different according to the thermal boundary conditions [19], it may be estimated approximately as

$$\frac{hd}{\lambda_f} = 4. \quad (54)$$

From equations (49) and (54),

$$\frac{q_w}{\tau_m} = \frac{4(\lambda_f/d)\Delta t}{8(\mu_f u_m/d)} = \frac{1}{2} Pr_f^{-1} \frac{g c_{p_f} \Delta t}{u_m}. \quad (55)$$

Substituting this into equation (38) and also into equation (39) gives

$$\frac{S_{ao}}{\tau_w} = \frac{1}{2}\left\{\left(\frac{1}{v}\frac{\mathrm{d}v}{\mathrm{d}i}\right)_m c_{p_f} \Delta t\right\} Pr_f^{-1} \quad (56)$$

for the general case, and

$$\frac{S_{ao}}{\tau_w} = \frac{1}{2}\frac{c_{p_f}}{c_{p_m}}\frac{\Delta T}{T_m} Pr_f^{-1} \quad (57)$$

for a perfect gas. Substituting these into equation (48), we obtain alternative formulas to discriminate the large effect of acceleration in case of heated laminar flow as

$$\left\{\left(\frac{1}{v}\frac{\mathrm{d}v}{\mathrm{d}i}\right)_m c_{p_f} \Delta t\right\} \geqslant 2Pr_f \quad (58)$$

for the general case, and as

$$\frac{c_{p_f}}{c_{p_m}}\frac{\Delta T}{T_m} \geqslant 2Pr_f \quad (59)$$

for the particular case of a perfect gas.

Hitherto, we dealt with the case of upward heated flow, where the characteristics of the phenomena are most pronounced. Now we briefly consider the distinctions between heated and cooled flows and also between upward and downward flows. The shearing-stress distribution near the wall is expressed by equation (15), where the values of S_{ao} and also of $[1-(\gamma_f/\gamma_m)]$ change their signs according to whether heated or cooled. Further, the sign attached to the buoyancy term changes according to the flow direction. Thus the shearing stress near the wall may decrease from τ_w in some case, while it may increase in another case. When it decreases, the treatment is quite the same as the case of upward heated flow mentioned hitherto. Therefore, equations (27), (29) and (51) are applicable to the case of downward cooled flow. On the other hand, when shearing stress near the wall increases from τ_w, the basic condition to discriminate the large effect may be expressed as

$$y_{\tau=3\tau_w} \leqq \delta_l \quad (60)$$

for turbulent flow, and as

$$y_{\tau=3\tau_w} \leqq \frac{R}{N} \quad (61)$$

for laminar flow. In these equations, $y_{\tau=3\tau_w}$ represents the point where τ amounts to $3\tau_w$ by linear extrapolation according to the gradient of τ at the wall. As a result, the conditions to discriminate the large effect of buoyancy for the case of upward cooled flow and also for that of downward heated flow are given as

$$2Re^{\frac{21}{8}} \leqslant 1{\cdot}55 \times 10^3\, Gr \qquad (Pr_f \leqslant 1) \quad (62)$$

$$2Re^{\frac{21}{8}} \leqslant 1{\cdot}55 \times 10^3\, Gr\, Pr_f^{-0{\cdot}4} \quad (Pr_f > 1) \quad (63)$$

for turbulent flow, and as

$$Gr\, Re^{-1} \geqslant 112 \quad (64)$$

for laminar flow. In these equations, the Grashof number is defined as $Gr = g[(\gamma_f - \gamma_m)/\gamma_f]d^3/\nu_f^2$ so that it may have a positive value. Lastly, as for the deceleration effect due to cooling, since $T_w < T_m$ in case of cooling, $|\Delta T/T| = |(T_w/T_m) - 1| < 1$ is approved. Therefore, from equations (44) and (57), $|S_{ao}/\tau_w|$ can hardly exceed a unity. As a result, neither the condition (60) nor condition (61) is satisfied in case of cooling. Thus the effect of deceleration due to cooling never occurs.

3.5 *Discussions on available measurements*

Supercritical fluids show very large volume changes near their critical temperatures and have considerably small kinematic viscosities. Thus it is expected that Grashof numbers for supercritical fluids come to very large and that the effect of buoyancy will become notable even for turbulent flow. Jackson and Evans-Lutterodt [20] and Shitsman [21] performed experiments of heat transfer for supercritical fluids in vertical tubes, by using carbon dioxide and water respectively. They compared the temperature distributions along the test tubes in case of upward flow with those in case of downward flow, under constant flow rates and constant heat fluxes. Their main results are reproduced in Figs. 1 and 2. Many anomalous phenomena have been observed concerning the heat transfer for supercritical fluids and are still under lively discussion [22]. However, the reason why the temperature distributions show such variations as shown in Figs. 1 and 2 according to the flow directions may be attributable to the effect of buoyancy. Thereupon, in Fig. 3 the experimental conditions in Figs. 1 and 2 are plotted against Reynolds number and Grashof number, and are compared with equation (27). It will be seen that equation (27) holds fairly good.

In connection with gas-cooled nuclear reactors and rocket propulsion systems, Taylor [9, 11, 12], DalleDonne and Bowditch [10], McEligot *et al.* [13], Perkins and Worsoe-Schmidt [14] and Lel'chuk *et al.* [15] performed

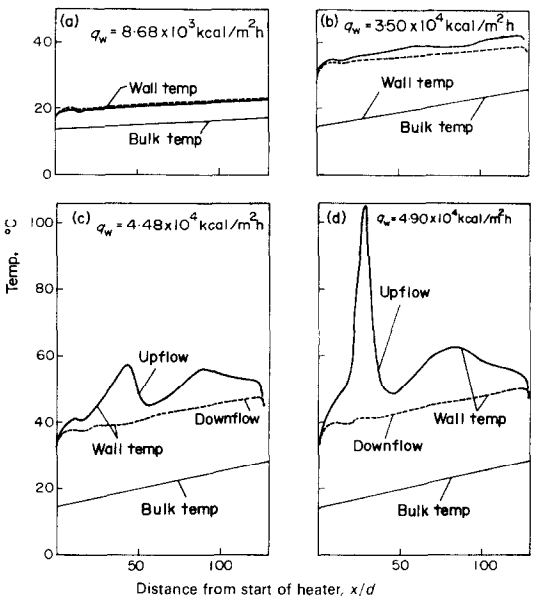

FIG. 1. Experimental wall temperature measurements for supercritical carbon dioxide [20]. $p = 77.3$ kg/cm², $d = 18.97$ mm, fluid inlet Reynolds number 1.13×10^5.

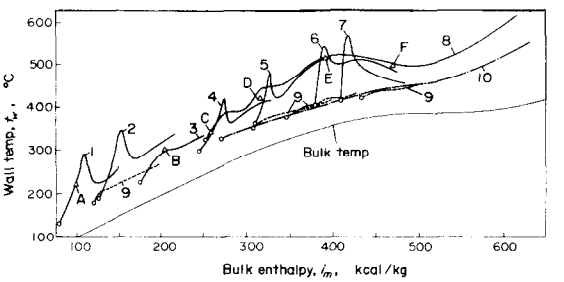

FIG. 2. Experimental wall temperature measurements at local bulk enthalpies for supercritical water [21].
$p = 250$ kg/cm².
Upflow:

1. $G = 389$ kg/m²s, $q_w = 3.09 \times 10^5$ kcal/m²h
2. 380 3.09
3. 386 2.80
4. 364 3.05 : $d = 16$ mm, $l/d = 100$.
5. 364 3.16
6. 362 2.94
7. 382 2.49
8. 375 2.99 : $d = 8$ mm, $l/d = 400$.

Downflow:

9. $G = 390$ kg/m²s, $q_w = 3.14 \times 10^5$ kcal/m²h : $d = 16$ mm, $l/d = 100$.
10. 354 3.01 : $d = 8$ mm, $l/d = 400$.

As for points A, B, ..., F, refer to Fig. 3.

experiments of turbulent heat and momentum transfer for gases in circular tubes at very high wall to bulk temperature ratios, by using air, hydrogen, nitrogen, helium and argon as test fluids. Among them, Taylor's data for helium were rearranged and are shown in Figs. 4 and 5. As for the momentum transfer, average friction coefficients had been calculated from the measured pressure drops between the inlet and the outlet of the test tube. The upper part of Fig. 4 is a plot of the average friction coefficients against the average Reynolds numbers for all the helium data in [9] and [12]. The line $f = 16/Re$ for laminar flow and Blasius' line for turbulent flow are also plotted in the figure. The lower part of Fig. 4 is a plot of $\Delta T/T_m = (T_w/T_m) - 1$, corresponding to the data in the upper part. The condition (46) to discriminate the large effect of acceleration in case of turbulent flow and also the condition (59) in case of laminar flow are also plotted in the figure. As for the heat transfer, local heat-transfer coefficients had been determined from the temperature measurements along the test tube. The upper part of Fig. 5 is a plot of the local Nusselt numbers against the local Reynolds numbers for runs 36, 40 and 42 in [12]. Dittus–Boelter's line is also plotted in the figure. The lower part of Fig. 5 is the same plot as in Fig. 4.

From Fig. 4, it is approved that when the experimental condition comes near the line represented by equation (46), the acceleration effect becomes prominent and results in a considerable increase of friction coefficient as explained in section 3.1. In contrast with this, from Fig. 5, the acceleration has only a slight effect on heat transfer. The reason may be explained as follows. The effects of acceleration and buoyancy firstly cause a considerable increase of the wall friction, which operates to decrease the thickness of the laminar sublayer. On the other hand, a steep negative gradient of shearing stress near the wall is also yielded and operates conversely to increase the thickness of the laminar sublayer. As a result of these opposing actions, the thickness of the laminar sublayer remains nearly unchanged from the usual case without the effects of acceleration and buoyancy.

4. TURBULENT BOUNDARY LAYER WITH FLUID-PROPERTY AND SHEARING-STRESS VARIATIONS

4.1 *Basic considerations*

From the discussions in the preceding chapters, a rapid decrease of shearing stress near the wall is yielded under the large effects of buoyancy and acceleration. At the same time, the fluid properties may vary considerably in the boundary layer. In several literatures [4, 7, 8], velocity and temperature profiles have been calculated for combined free and forced laminar flow in vertical circular tubes. As for turbulent flow, however, the theory of turbulence is not yet well in hand even for adiabatic, fully developed, pipe flow. Under these circumstances, the authors expect to propose an approximate theory to calculate velocity and temperature profiles under the large effects of buoyancy and acceleration.

Basic equations for turbulent momentum and heat transfer are expressed as

$$\tau = (\nu + \varepsilon_m)\frac{\gamma}{g}\frac{\partial u}{\partial y}, \tag{65}$$

$$q = -(\lambda + \gamma c_p \varepsilon_t)\frac{\partial t}{\partial y} = -\left(\frac{\nu}{Pr} + \frac{\varepsilon_m}{Pr_t}\right)\gamma c_p \frac{\partial t}{\partial y}. \tag{66}$$

At the beginning, the usual theory of turbulent heat transfer will be briefly reviewed. By defining

$$y^+ = \frac{\sqrt{(g\tau_w/\gamma)}}{\nu}y, \qquad u^+ = \frac{u}{\sqrt{(g\tau_w/\gamma)}}, \tag{67}$$

a so-called wall law holds true for the velocity distribution:

$$u^+ = \phi(y^+). \tag{68}$$

From equations (65) and (67),

$$\left(1 + \frac{\varepsilon_m}{\nu}\right)\frac{du^+}{dy^+} = \frac{\tau}{\tau_w} \doteqdot 1. \tag{69}$$

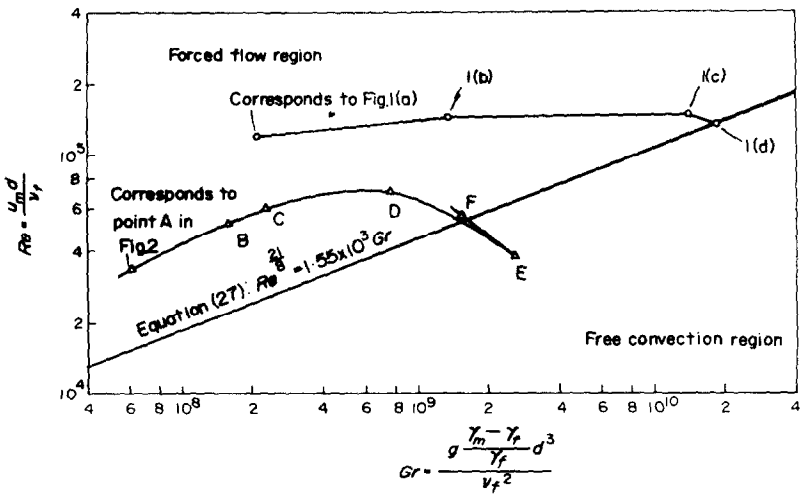

FIG. 3. Comparison of the prediction of equation (27) for experimental data in Figs. 1 and 2.

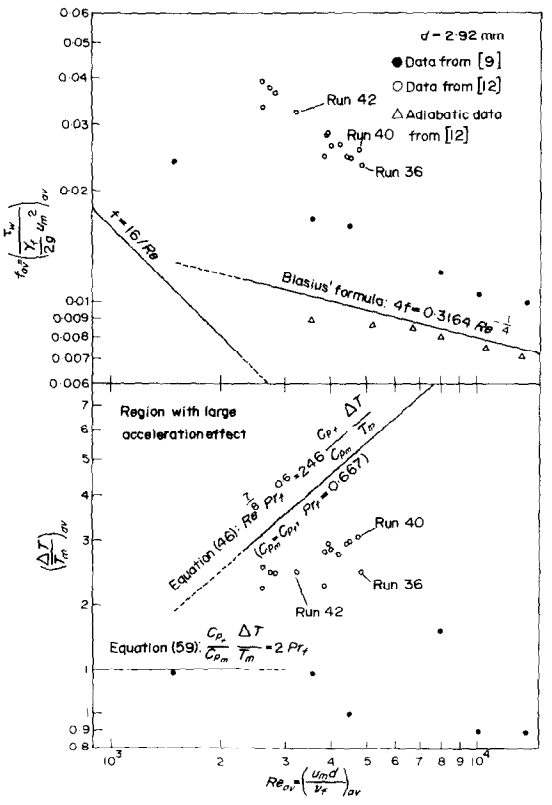

FIG. 4. Average friction coefficients for helium flowing in a tube at very high wall to bulk temperature ratios [9, 12].

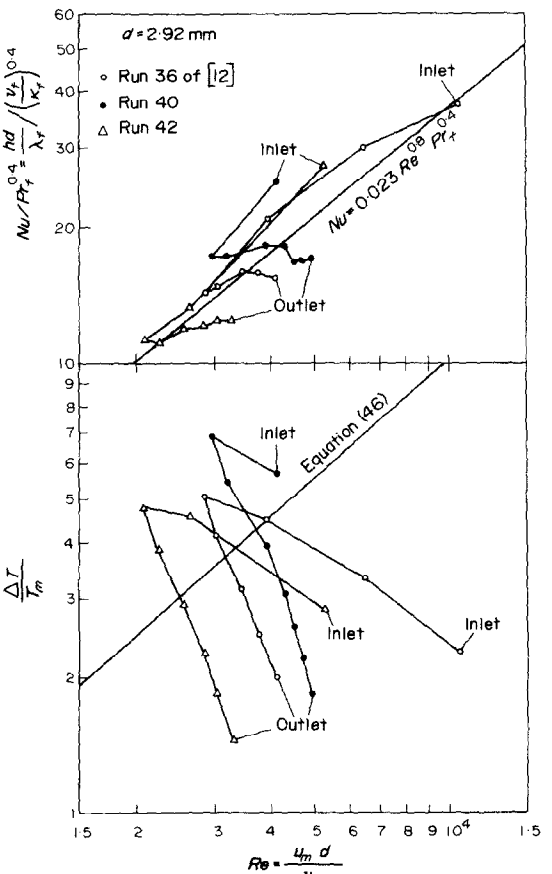

FIG. 5. Local heat-transfer coefficients for helium flowing in a tube at very high wall to bulk temperature ratios [12].

From equations (68) and (69), the eddy diffusivity for momentum is determined as

$$\frac{\varepsilon_m}{\nu} = \frac{1}{\mathrm{d}\phi/\mathrm{d}y^+} - 1 = \psi(y^+). \tag{70}$$

Usually it is assumed that $Pr_f = \varepsilon_m/\varepsilon_t = 1$ for the turbulent Prandtl number. Then, introducing a proper heat-flux distribution into the energy equation (66) and integrating yield a temperature distribution.

The authors [1, 2] have been studying the turbulent heat transfer to supercritical fluids, whose properties vary extremely with temperature. The turbulent boundary layer with large variation of fluid properties was first studied by Deissler [23] and by Goldmann [24] in respective ways of approach. In [1], the authors were incited by Goldmann's work. His theory assumes that the turbulent mixing process at any point—that is, the growth and damping of turbulent eddies—is a function of the fluid properties at that point. Then it is assumed that the universal turbulent-velocity profile of equation (68), which has been verified for isothermal flow, may be used to describe non-isothermal flow fields with variable properties, provided the velocity and distance parameters are defined by

$$y^{++} = \int_0^y \frac{\sqrt{[g\tau_w/\gamma(y)]}}{\nu(y)}\,\mathrm{d}y,$$

$$u^{++} = \int_0^u \frac{\mathrm{d}u}{\sqrt{[g\tau_w/\gamma(y)]}}. \tag{71}$$

Thus,

$$u^{++} = \phi(y^{++}). \tag{72}$$

From equations (65) and (71), the relation quite similar to equation (69) is obtained:

$$\left(1 + \frac{\varepsilon_m}{\nu}\right)\frac{\mathrm{d}u^{++}}{\mathrm{d}y^{++}} = \frac{\tau}{\tau_w} \doteqdot 1. \tag{73}$$

Therefore, Goldmann's assumption is translated into an assumption in terms of eddy diffusivity; that is, when the dimensionless distance is defined as equation (71), the expression (70) for the distribution of eddy diffusivity in the case of constant fluid properties can be applied as is to the case of varying fluid properties:

$$\frac{\varepsilon_m}{\nu} = \psi(y^{++}). \tag{74}$$

As mentioned at the beginning of this section, the shearing stress changes considerably in the turbulent boundary layer under the large effects of buoyancy and acceleration. A similar situation happens in case of flow in falling liquid films (where the variation of fluid properties need not be considered). In such cases, the approximation that $\tau \doteqdot \tau_w$ in the boundary layer, which was assumed in deriving equation (70) from equation (69), can no longer be applied. Thus, the consequent velocity profiles differ from each other according to which formula we may adopt as the basic wall law from among equations (68) and (70). Dukler and Bergelin [25], Seban [26] and Rohsenow *et al.* [27] adopted the universal velocity profile (68) itself as the basic law and calculated the characteristics of flow in falling liquid films. On the other hand, Dukler [28] and Davis [29] assumed the expression (70) for eddy diffusivity to be fundamental and calculated the velocity profiles and other characteristics of flow in falling liquid films.

As for the present case where both the shearing stress and the fluid properties change in the boundary layer, the authors assume as follows, by combining Goldmann's theory [24] in case of varying fluid properties with Dukler's theory [28] in case of varying shearing stress. Namely, the authors assume the expression (70) for eddy diffusivity as the basic representation of the wall law. Equation (71) due to Goldmann defines the distance parameter y^{++} in case of varying fluid properties as an integrated mean value of y^+ by taking into consideration the variation of kinematic viscosity and that of shearing-stress velocity (in this case, the variation of shearing-stress velocity results only from the density variation). When the shearing stress also changes,

the authors now define the dimensionless distance y^* as

$$y^* = \int_0^y \frac{\sqrt{[g|\tau(y)|/\gamma(y)]}}{\nu(y)}\,dy \tag{75}$$

and assume that the expression (70) for eddy diffusivity in the case of constant fluid properties may be applied as is to the case with fluid-property and shearing-stress variations:

$$\frac{\varepsilon_m}{\nu} = \psi(y^*). \tag{76}$$

This assumption is easily translated into an assumption in terms of velocity profile as follows. By making a pair with equation (75), we define

$$u^* = \int_0^u \frac{|du|}{\sqrt{[g|\tau(y)|/\gamma(y)]}}. \tag{77}$$

Then, from equations (65), (75) and (77), we have the following relation quite similar to equation (69).

$$\left(1 + \frac{\varepsilon_m}{\nu}\right)\frac{du^*}{dy^*} = 1. \tag{78}$$

Since we assumed for the eddy diffusivity equation (76) which has the same form as equation (70), integrating equation (78) yields the same relation as equation (68) between u^* and y^*;

$$u^* = \phi(y^*). \tag{79}$$

4.2 *Computation procedure*

We have obtained equations (65), (66), (75) and (76) for the basic equations of the turbulent boundary layer with large variations of fluid properties and shearing stress. Further, equations (4), (5), (8), (9) and (12) hold for the shearing-stress distribution. In solving these equations, we assume that $Pr_t = \varepsilon_m/\varepsilon_t = 1$ and that

$$q = q_w\left(1 - \frac{y}{R}\right) \tag{80}$$

for the heat-flux distribution. For the convenience of practising numerical integrations, equations (65), (66), (75), (76), (8), (9) and (12) are transformed as follows.

$$\frac{du}{dy} = \frac{g\tau/\gamma}{\nu(1 + \varepsilon_m/\nu)}, \tag{81}$$

$$\frac{dt}{dy} = \frac{-q_w(1 - y/R)}{\lambda + g\mu c_p(\varepsilon_m/\nu)}, \tag{82}$$

$$\frac{dy^*}{dy} = \frac{\sqrt{[g|\tau|/\gamma]}}{\nu}, \tag{83}$$

$$\frac{\varepsilon_m}{\nu} = \psi(y^*), \tag{84}$$

$$\frac{dS_a}{dy} = \frac{1}{g}\frac{1}{u_m}\frac{du_m}{dx}\gamma u^2\left(1 - \frac{y}{R}\right), \tag{85}$$

$$\frac{dS_g}{dy} = \gamma\left(1 - \frac{y}{R}\right), \tag{86}$$

$$\tau = -\left(\frac{R}{R-y} - \frac{R-y}{R}\right)(S_{ao} + S_{go}) + \frac{R}{R-y}(S_a + S_g) + \frac{R-y}{R}\tau_w. \tag{87}$$

In order to calculate the flow rate W and the total enthalpy flow rate I simultaneously, we set

$$\frac{dW'}{dy} = 2\pi(R - y)\gamma u, \tag{88}$$

$$\frac{dI'}{dy} = 2\pi(R - y)\gamma u i \tag{89}$$

where W' and I' represent respectively the flow rate and the total enthalpy flow rate across the annular section between the radii of R and $R - y$. The equations (81)–(89) constitute a system of simultaneous ordinary differential equations about u, t, y^*, S_a, S_g, W' and I'. When the heat flux q_w at the wall, the skin friction τ_w, and the wall temperature t_w are given, these equations can be solved by the following procedure. By assuming suitable values for $(1/u_m) \times (du_m/dx)$ in equation (85) and for $(S_{ao} + S_{go})$ in equation (87), we can integrate the above equations numerically under the boundary

conditions:

$$y = 0; u = 0, t = t_w, y^* = S_a = S_g = W' = I' = 0 \quad (90)$$

at the wall. Then we obtain the velocity profile, the temperature profile, the flow rate:

$$W = W'(y = R), \quad (91)$$

the bulk enthalpy:

$$i_m = I'(y = R)/W \quad (92)$$

and others. If the assumed values for $1/u_m\, du_m/dx$ and for $(S_{ao} + S_{go})$ are proper, we may have the following balances; first, by substituting the integrated results into the right-hand side of equation (35):

$$\frac{1}{u_m}\frac{du_m}{dx} = \left(\frac{dv}{di}\right)_m \frac{4q_w}{du_m} = \left(\frac{1}{v}\frac{dv}{di}\right)_m \frac{\pi dq_w}{W} \quad (93)$$

and second, according to equations (4) and (5):

$$S_{ao} + S_{go} = S_a(y = R) + S_g(y = R). \quad (94)$$

If these balances do not hold, we modify the values for $(1/u_m)(du_m/dx)$ and for $(S_{ao} + S_{go})$ in a proper manner. Thus we attain to the final solution by successive approximations. It will be worth while to go into some details of practical computations. The initial values for $(1/u_m) \times (du_m/dx)$ and for $(S_{ao} + S_{go})$ were determined from the solution for the case without the effects of buoyancy and acceleration, that is, the case: $\tau = [1 - (y/R)]\tau_w$. It follows from equation (87) that when the balance (94) does not hold the value of τ diverges with an order $R/(R - y)$ according as $y \to R$. As mentioned in Section 2, however, it is known that the actual shearing stress converges linearly to zero. Therefore, we interrupted the calculation of τ from equation (87) at a certain point, and estimated τ by linear interpolation from that point to the centre.

Several expressions have been proposed as for the distribution of eddy diffusivity. Whichever expression we may adopt, the computed results differ only slightly from one another. The authors adopted the following Reichardt's formula [30] in the succeeding section.

$$\frac{\varepsilon_m}{\nu} = \kappa y_n^+ \left(\frac{y^*}{y_n^+} - \tanh\frac{y^*}{y_n^+} - \frac{1}{3}\tanh^3\frac{y^*}{y_n^+}\right) \quad (95)$$

where $\kappa = 0{\cdot}4$ and $y_n^+ = 7{\cdot}15$. The computations were performed by HITAC 5020E computer of the Data Processing Center in the University of Tokyo.

4.3 *Comparison between computed and experimental results*

By the procedure mentioned above, the acceleration effect was theoretically calculated for the case of turbulent heat and momentum transfer for air in a circular tube at large wall to bulk temperature ratios. The physical properties of air were referred to the appendix of [19]. The computed results are illustrated in Figs. 6(a), (b) and (c), in the same manner as Figs. 4 and 5. As explained in the preceding section, a given set of wall temperature t_w, heat flux q_w and skin friction τ_w determines a corresponding solution. Thus, in Fig. 6, results are shown for various wall heat fluxes q_w under a constant wall temperature of $t_w = 1800°C$. Although these results for air cannot be compared with those in Figs. 4 and 5 for helium in a strict sense, similar inclinations are obvious; that is, the friction coefficient increases greatly as $\Delta T/T_m$ comes near to the line of equation (46), while the heat-transfer coefficient changes only slightly. At this juncture, as $\Delta T/T_m$ gets small, the convective state draws towards the usual turbulent convection with constant fluid properties. Then the computed results should tend either to Blasius' line or to Dittus–Boelter's line. In Fig. 6, however, the computed values for $\Delta T/T_m \to 0$ show slight deviations from Blasius' line or Dittus–Boelter's line according as Reynolds number comes to small. A 'non-turbulent region' shown in Fig. 6 (c) will be explained in the next section and so will Fig. 6(d). In Fig. 7, the distributions of shearing stress, velocity and temperature in the tube are shown for the case: $Re = 6{\cdot}33 \times 10^3$ and $\Delta T/T_m = 2{\cdot}17$.

As for the buoyancy effect, theoretical com-

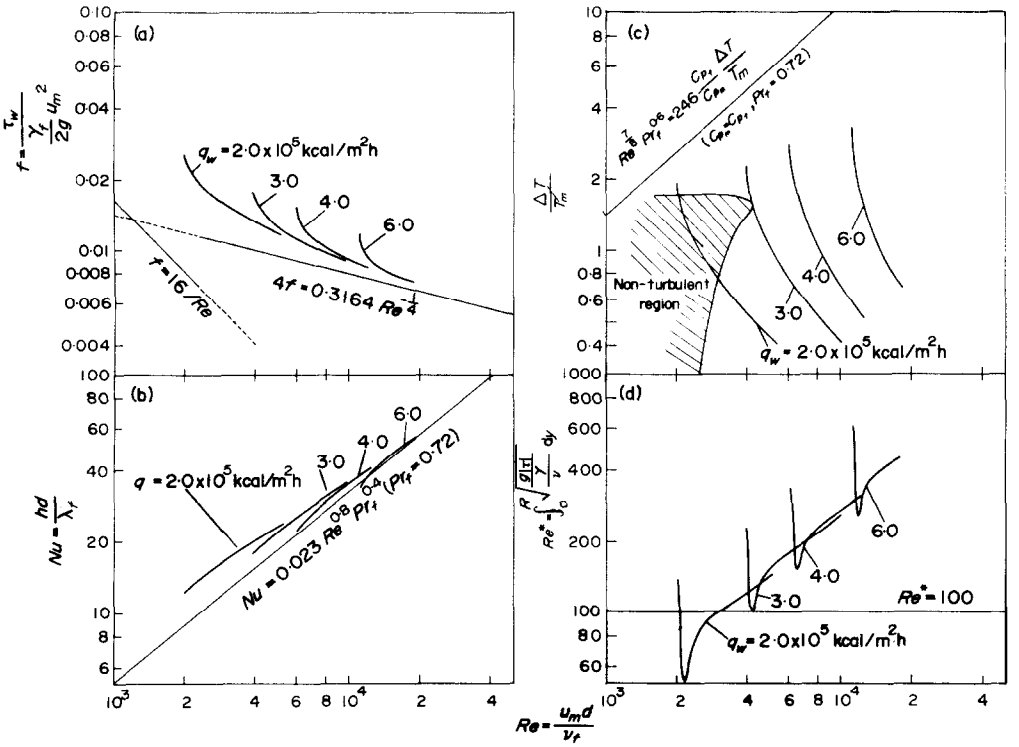

FIG. 6. Computed results of the acceleration effect for air flowing in a tube. $p = 1$ atm, $d = 6$ mm, $t_w = 1800$°C.

putations were performed for the same conditions as Shitsman's experiments shown in Fig. 2. The physical properties of water were referred to [31]. The lower part of Fig. 8 shows the computed results for wall temperature, and the upper part of Fig. 8 shows the results for skin friction. As compared with the experimental ones in Fig. 2, the computed wall temperatures show an opposite tendency dependent on flow directions. Thus, the theory is not sufficient to estimate heat-transfer coefficients. On the other hand, the computed skin friction for upward flow reaches to about ten times as large as that for downward flow in an extreme case, though experimental values are not available. As explained in Sections 3.1 and 3.5, the effects of buoyancy and acceleration primarily bring about a large increase of skin friction, while their influence on heat transfer consists of two opposing factors (one of which acts to promote, and another acts to suppress heat transfer) to make itself secondary and difficult to estimate. In addition, the property variation of supercritical fluid is quite anomalous. The authors think that the computed results for heat transfer were unsatisfactory for these two reasons. From among the results in Fig. 8, Fig. 9 demonstrates the differences of shearing-stress, velocity and temperature distributions between upward and downward flows under a constant bulk enthalpy of $i_m = 415$ kcal/kg.

4.4 *Reverse transition from turbulent to laminar flow*

Wilson and Pope [32] noted that heat-transfer coefficients on the convex side of a gas-turbine blade were considerably lower than anticipated for a turbulent boundary layer. They suggested that acceleration may have caused the boundary layer to return from turbu-

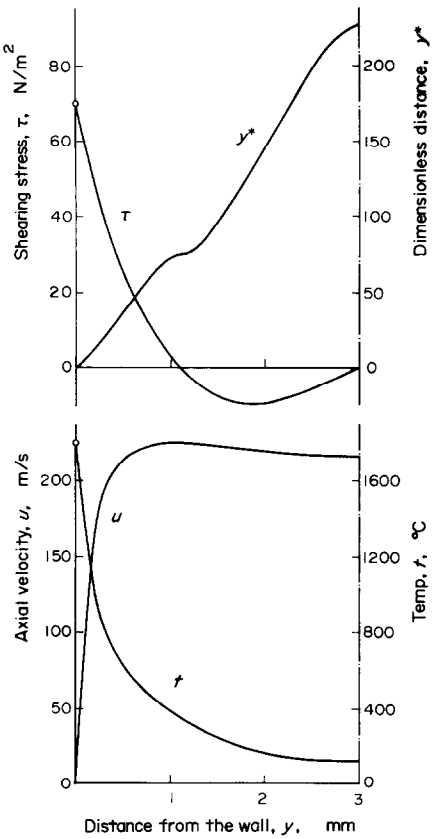

FIG. 7. An example of theoretical distributions of shearing stress, velocity and temperature for air flowing in a tube at a very high wall to bulk temperature ratio. $p = 1$ atm, $d = 6$ mm, $t_w = 1800°C$, $q_w = 4{\cdot}0 \times 10^5$ kcal/m²h, $\tau_w = 70$ N/m², $G = 1{\cdot}10 \times 10^2$ kg/m²s, $Re = 6{\cdot}33 \times 10^3$, $t_m = 381°C$, $\Delta T/T_m = 2{\cdot}17$, $Gr_a = 2{\cdot}01 \times 10^6$, $f = 0{\cdot}0131$, $Nu = 23{\cdot}7$.

lent to laminar. This phenomenon of the reverse transition has been attracting increasing interest in recent years. Many experiments have been performed mainly for the case of accelerated flows in convergent channels [33–37], and partly for the case of highly heated gas flows in circular tubes where the flows are accelerated by thermal expansion [38, 39]. Moretti and Kays [33] and Patal and Head [34], by arranging their own experiments for convergent channels, proposed respective empirical formulas to discriminate the onset of a reverse transition. Most of the subsequent literatures have followed Moretti's formula, which claims that the reverse transition will take place when a dimensionless acceleration parameter K defined in the following equation satisfies

$$K \equiv \frac{\nu}{u_m^2}\frac{du_m}{dx} = 3{\cdot}5 \times 10^{-6}. \qquad (96)$$

On the other hand, Patal's formula claims that the transition occurs when a dimensionless gradient Δ_τ of shearing stress at the wall satisfies

$$\Delta_{\tau_w} \equiv \frac{\nu}{(\gamma/g)(g\tau_w/\gamma)^{\frac{3}{2}}}\frac{d\tau}{dy} = -0{\cdot}009. \qquad (97)$$

Bradshaw [40] considered that in order that a boundary layer remains turbulent there shall

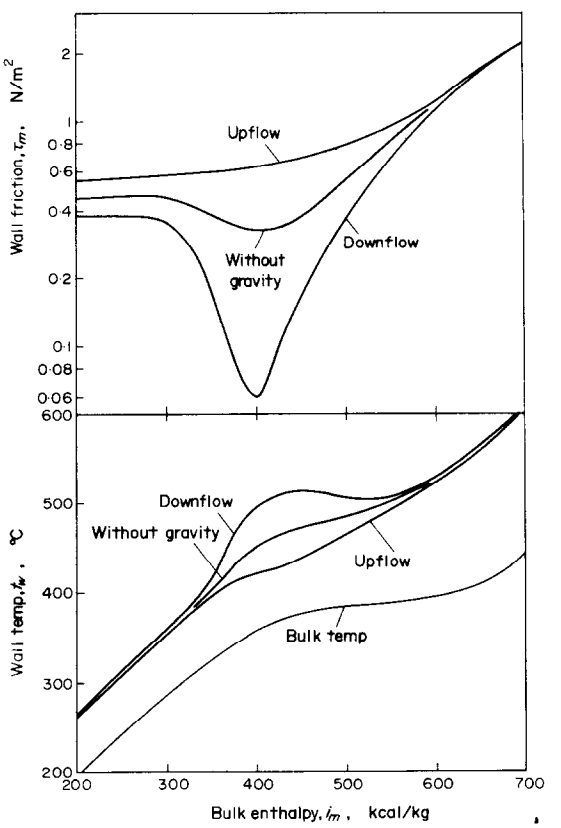

FIG. 8. Computed results of the buoyancy effect for the case of heat transfer to supercritical water shown in Fig. 2. $p = 250$ kg/cm², $d = 16$ mm, $G = 380$ kg/m²s, $q_w = 3{\cdot}09 \times 10^5$ kcal/m²h.

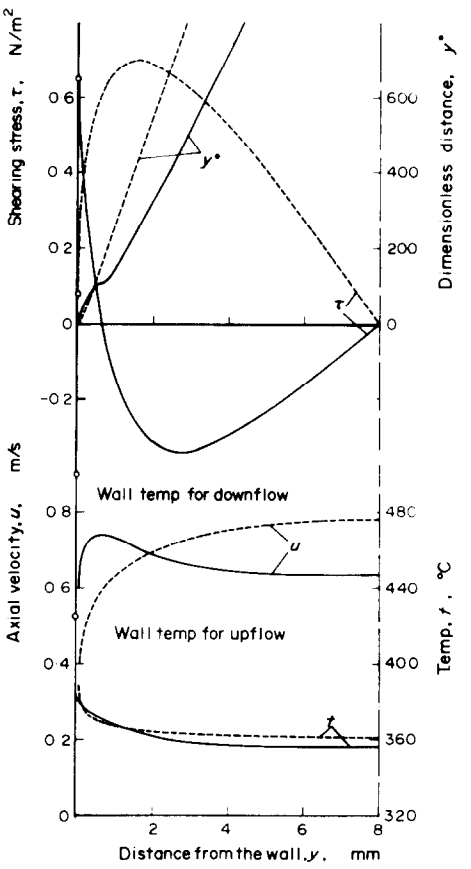

FIG. 9. Comparison between upward and downward flows for shearing-stress, velocity and temperature distributions in case of heat transfer to supercritical water. $p = 250\,\text{kg/cm}^2$, $d = 16\,\text{mm}$, $G = 380\ \text{kg/m}^2\text{s}$, $q_w = 3{\cdot}09 \times 10^5\ \text{kcal/m}^2\text{h}$, $i_m = 415\ \text{kcal/kg}$; ———: upflow, $Re = 5{\cdot}95 \times 10^4$, $Gr = 2{\cdot}82 \times 10^9$; - - - -: downflow, $Re = 4{\cdot}19 \times 10^4$, $Gr = 2{\cdot}35 \times 10^9$.

be some region of the boundary layer where the energy containing and dissipating ranges of eddy size do not quite overlap. By assuming that the reverse transition occurs when this viscosity-independent region shrinks and vanishes, he argued the critical Reynolds number for usual flow in circular tubes and also Patal's criterion mentioned above. Apart from the reverse transition due to acceleration, Hall *et al.* [22, 41] noticed the local deterioration of heat transfer which was observed in the experiments for supercritical fluids performed by themselves (see Fig. 1) and also by Shitsman [42]. They investigated the shearing-stress distribution near the wall by taking the buoyancy force into consideration, and explained the deterioration of heat transfer by a reduction of turbulence energy generation in the turbulent boundary layer.

In this paper, the authors have discussed the effects of boyancy and acceleration from a somewhat different point of view. Recent studies cited above, however, insist that the effects of buoyancy and acceleration bring about a reverse transition when a certain condition is satisfied. Now the authors want to discuss in this relation. As for the usual flow in circular tubes, a turbulent convection appears when Reynolds number exceeds 2300. Then the dimensionless distance y^+ defined by equation (67) has to satisfy $Re^+ \equiv y^+_{y=R} = \sqrt{(g\tau_w/\gamma)}\,R/\nu \geqslant 150$ at the centre of the tube. By taking into account that the shearing stress decreases linearly to zero at the centre, the above relation is converted into the relation $Re^* \equiv y^*_{y=R} \geqslant 100$ in terms of y^* defined by equation (75). As for the case with large variations of fluid properties and of shearing stress, it seems natural to assume that a turbulent convection is maintained when

$$Re^* \equiv y^*_{y=R} = \int_0^R \frac{\sqrt{(g|\tau|/\gamma)}}{\nu}\,dy \geqslant 100. \quad (98)$$

Concerning Fig. 6 in the preceding section, computed values of Re^* are also plotted in Fig. 6 (d). From this figure, a 'non-turbulent region' shown in Fig. 6 (c) is determined. It is expected that a reverse transition may take place in the range $Re < 4300$ when a certain heating condition is satisfied. At this juncture, it is noticeable that, in the case of flow in circular tubes, a factor $[1 - (u_f^2/u_m^2)(\gamma_f/\gamma_m)]$ in the acceleration term and a factor $[1 - (\gamma_f/\gamma_m)]$ in the buoyancy term of equation (14) relate closely the shearing-stress distribution with the temperature distribution, and that the shearing stress may continue to decrease to a fairly large

negative value even after it vanishes and changes its sign, as shown in Figs. 7 and 9. For this reason, Re^* cannot become effectively small in the case of flow in circular tubes, and a reverse transition occurs only in the limited region where Reynolds number does not largely exceed 2300. In contrast with this, it is expected that, in the case of accelerated flow in convergent channels, the shearing stress never changes its sign even if it decreases greatly near the wall, and that Re^* becomes effectively small to bring about a reverse transition even in the region of fairly high Reynolds number.

In order to determine exactly the region where condition (98) is satisfied, considerable numerical computations are required as explained concerning Fig. 6. After some considerations, however, it is roughly expected that the condition $Re^* = 100$ may be well satisfied in the neighbourhood of the boundary line where the equal sign holds in the various formulas in the preceding chapter to discriminate the large effects of buoyancy and acceleration. At this juncture, equation (33) to discriminate the large effect of acceleration can be transformed by using Moretti's parameter K as

$$K \geqslant 6{\cdot}45 \times 10^{-4}\, Re^{-\frac{1}{8}} \frac{\gamma_f}{\gamma_m}. \qquad (99)$$

It is noticeable that when $Re = 1 \times 10^5$ and $\gamma_m = \gamma_f$ for isothermal accelerated flow, the right-hand side of equation (99) amounts to $8{\cdot}6 \times 10^{-6}$, which fairly agrees with the empirical equation (96). Further, Patal's parameter is written as

$$\Delta_\tau = \frac{\nu}{(\gamma/g)\,(g\tau_w/\gamma)^{\frac{1}{2}}} \frac{\mathrm{d}\tau}{\mathrm{d}y} = \frac{\mathrm{d}\tau/\tau_w}{\mathrm{d}y^+}. \qquad (100)$$

Then Patal's formula (97) is proved to insist that a reverse transition occurs when

$$y^+_{\tau=0} \equiv \sqrt{\left(\frac{g\tau_w}{\gamma}\right)}\, y_{\tau=0}/\nu = \frac{1}{0{\cdot}009} = 111$$

in terms of the authors' notation. Although this value of 111 seems somewhat too large, Patal's formula can ultimately be transformed into an equation quite similar (only with a different numerical coefficient) to those in the preceding chapter.

In conclusion, the effects of buoyancy and acceleration become predominant when the formulas obtained in the preceding chapter are satisfied. When Reynolds number is not so greater than 2300, however, a reverse transition from turbulent to laminar flow takes place just near where the equal sign in those formulas holds.

5. CONCLUSIONS

In this paper, the authors discussed the shearing-stress distribution in case of forced turbulent convection in vertically placed tubes, by taking into account the effects of buoyancy and of acceleration due to thermal expansion. It was proved that the effects of buoyancy and of acceleration act quite similarly and result in a very rapid decrease of the shearing stress near the wall. By considering how the velocity profile is affected by the shearing-stress gradient near the wall, the authors deduced the formulas (27) and (29) to discriminate the large effect of buoyancy, and also the formulas (33), (45) and (46) to discriminate the large effect of acceleration. These formulas were compared with the available experimental data. It was also proved that the effects of buoyancy and acceleration primarily bring about a great increase of skin friction, while they have only a slight influence on heat transfer. Further, the case of laminar flow and the distinctions between upward and downward flows and also between heated and cooled flows were discussed.

When the effects of buoyancy and acceleration become predominant, not only the shearing stress but the fluid properties often show extreme variations near the wall. The authors proposed an approximate theory to calculate velocity and temperature profiles under these circumstances, by assuming that the turbulent boundary layer is constructed by the superposition of the locally developed layers. The

theoretical results were compared with the experimental ones.

A phenomenon of a reverse transition from turbulent to laminar flow was also considered. Based on the above theory, a new criterion of a reverse transition was proposed.

REFERENCES

1. H. TANAKA, N. NISHIWAKI and M. HIRATA, Turbulent heat transfer to supercritical carbon dioxide, *Proc. Japan Soc. Mech. Engrs Semi-Int. Symp., Tokyo, Heat Mass Transfer*, Vol. 2, p. 127 (1967).
2. H. TANAKA, N. NISHIWAKI, M. HIRATA and A. TSUGE, Forced convection heat transfer to fluid near critical point flowing in circular tube, *Int. J. Heat Mass Transfer* **14**, 739 (1971).
3. E. R. G. ECKERT and A. J. DIAGUILA, Convective heat transfer for mixed, free, and forced flow through tubes, *Trans. Am. Soc. Mech. Engrs* **76**, 497 (1954).
4. L. N. TAO, On combined free and forced convection in channels, *J. Heat Transfer* **82**, 233 (1960).
5. G. A. KEMENY and E. V. SOMERS, Combined free and forced-convective flow in vertical circular tubes—Experiments with water and oil, *J. Heat Transfer* **84**, 339 (1962).
6. B. METAIS and E. R. G. ECKERT, Forced, mixed and free convection regimes. *J. Heat Transfer* **86**, 295 (1964).
7. M. IQBAL and J. W. STACHIEWICZ, Influence of tube orientation on combined free and forced laminar convection heat transfer, *J. Heat Transfer* **88**, 109 (1966).
8. M. IQBAL, S. A. ANSARI and B. D. AGGARWALA, Effect of buoyancy on forced convection in vertical regular poligonal ducts, *J. Heat Transfer* **92**, 237 (1970).
9. M. F. TAYLOR and T. A. KIRCHGESSNER, Measurements of heat transfer and friction coefficients for helium flowing in a tube at surface temperatures up to 5900°R, NASA TN D-133, (1959).
10. M. DALLEDONNE and F. H. BOWDITCH, High temperature heat transfer: Local heat transfer and average friction coefficients for subsonic laminar, transitional and turbulent flow of air in a tube at high temperature, *Nucl. Engng* **8**, 20 (1963).
11. M. F. TAYLOR, Experimental local heat-transfer and average friction data for hydrogen and helium flowing in a tube at surface temperatures up to 5600°R, NASA TN D-2280, (1964).
12. M. F. TAYLOR, Experimental local heat-transfer data for precooled hydrogen and helium at surface temperatures up to 5300°R, NASA TN D-2595, (1965).
13. D. M. MCELIGOT, P. M. MAGEE and G. LEPPERT, Effect of large temperature gradients on convective heat transfer: The downstream region, *J. Heat Transfer* **87**, 67 (1965).
14. H. C. PERKINS and P. WORSØE-SCHMIDT, Turbulent heat and momentum transfer for gases in a circular tube at wall to bulk temperature ratios to seven, *Int. J. Heat Mass Transfer* **8**, 1011 (1965).
15. V. L. LEL'CHUK, K. F. SHUISKAYA and A. G. SOROKIN, Turbulent heat transfer of argon flowing in pipes under wall-temperatures up to 3000°K, Proc. 4th Int. Heat Transfer Conf., Paris, Vol. 2, Paper No. FC4.2, (1970).
16. D. M. MCELIGOT, S. B. SMITH and C. A. BANKSTON, Quasi-developed turbulent pipe flow with heat transfer, *J. Heat Transfer* **92**, 641 (1970).
17. L. V. HUMBLE, W. H. LOWDERMILK and L. G. DESMON, Measurements of average heat-transfer and friction coefficients for subsonic flow of air in smooth tubes at high surface and fluid temperatures, NACA Rep. 1020, (1951).
18. YOSHIRO KATTO, *Outlines of Heat Transfer* (in Japanese), p. 103. Yokendo, Tokyo (1968).
19. E. R. G. ECKERT and R. M. DRAKE, JR., *Heat and Mass Transfer*, 2nd ed., pp. 204, 190. McGraw-Hill, New York (1959).
20. J. D. JACKSON and K. EVANS-LUTTERODT, Impairment of turbulent forced convection heat transfer to supercritical pressure CO_2 caused by buoyancy forces, Research Rept., N.E.2, Dept. Nuclear Engng, Univ. Manchester, (1968).
21. M. E. SHITSMAN, Natural convection effect on heat transfer to a turbulent water flow in intensively heated tubes at supercritical pressure, *Proc. Inst. Mech. Engrs* **182**, Pt. 3I, 36 (1967–68).
22. W. B. HALL, J. D. JACKSON and A. WATSON, A review of forced convection heat transfer to fluids at supercritical pressures, *Proc. Inst. Mech. Engrs* **182**, Pt. 3I, 10 (1967–68).
23. R. G. DEISSLER, Heat transfer and fluid friction for fully developed turbulent flow of air and supercritical water with variable fluid properties, *Trans. Am. Soc. Mech. Engrs* **76**, 73 (1954).
24. K. GOLDMANN, Heat transfer to supercritical water and other fluids with temperature-dependent properties, *Chem. Engng Prog. Symp. Ser.* **50** (11), 105 (1954).
25. A. E. DUKLER and O. P. BERGELIN, Characteristics of flow in falling liquid films, *Chem. Engng Prog.* **48** (11), 557 (1952).
26. R. A. SEBAN, Remarks on film condensation with turbulent flow, *Trans. Am. Soc. Mech. Engrs* **76**, 299 (1954).
27. W. M. ROHSENOW, J. H. WEBBER and A. T. LING, Effect of vapor velocity on laminar and turbulent-film condensation, *Trans. Am. Soc. Mech. Engrs* **78**, 1637 (1956).
28. A. E. DUKLER, Fluid mechanics and heat transfer in vertical falling-film system, *Chem. Engng Prog. Symp. Ser.* **56** (30), 1 (1960).
29. E. J. DAVIS, An analysis of liquid film flow, *Chem. Engng Sci.* **20**, 265 (1965).
30. H. REICHARDT, Vollständige Darstellung der turbulenten Geschwindigkeits-Verteilung in glatten Leitungen, *Z. Angew. Math. Mech.* **31** (7), 208 (1951); and *Recent Advances in Heat and Mass Transfer*, edited by J. P. HARTNETT, p. 223. McGraw-Hill, New York (1961).
31. *JSME Steam Tables*, Japan Soc. Mech. Engrs, Tokyo (1968).
32. D. G. WILSON and J. A. POPE, Convective heat transfer

to gas turbine blade surfaces, *Proc. Inst. Mech. Engrs* **168**, 861 (1954).
33. P. M. MORETTI and W. M. KAYS, Heat transfer to a turbulent boundary layer with varying free-stream velocity and varying surface temperature—An experimental study, *Int. J. Heat Mass Transfer* **8**, 1187 (1965).
34. V. C. PATAL and M. R. HEAD, Reversion of turbulent to laminar flow, *J. Fluid Mech.* **34**, 371 (1968).
35. M. A. BADRI NARAYANAN and V. RAMJEE, On the criteria for reverse transition in a two-dimensional boundary layer flow, *J. Fluid Mech.* **35**, 225 (1969).
36. L. H. BACK, R. F. CUFFEL and P. F. MASSIER, Laminarization of a turbulent boundary layer in nozzle-flow—Boundary layer and heat transfer measurements with wall cooling, *J. Heat Transfer* **92**, 333 (1970).
37. W. M. KAYS, R. J. MOFFAT and W. H. THIELBAHR, Heat transfer to the highly accelerated turbulent boundary layer with and without mass addition, *J. Heat Transfer* **92**, 499 (1970).
38. C. W. COON and H. C. PERKINS, Transition from the turbulent to the laminar regime for internal convective flow with large property variations, *J. Heat Transfer* **92**, 506 (1970).
39. C. A. BANKSTON, The transition from turbulent to laminar gas flow in a heated pipe, *J. Heat Transfer* **92**, 569 (1970).
40. P. BRADSHAW, A note on reverse transition, *J. Fluid Mech.* **35**, 387 (1969).
41. W. B. HALL, The effect of buoyancy forces on forced convection heat transfer in a vertical pipe, Research Rept., N.E.1, Dept. Nuclear Engng, Univ. Manchester, (1968).
42. M. E. SHITSMAN, Impairment of the heat transmission at supercritical pressures, *Teplofiz. Vysokikh Temperature* **1** (1963).
43. A. B. CAMBEL and B. H. JENNINGS, *Gas Dynamics*, p. 83. McGraw-Hill, New York (1958).

APPENDIX

For the case of high speed flow, a relation corresponding to equation (38) will be introduced. At this juncture, we have to consider the volume change due to pressure drop with regard to the continuity equation, and also the kinetic energy with regard to the energy equation. For the sake of brevity, we deal with a perfect gas and assume that c_p = const. As basic equations, we first have equation (34) for continuity. By substituting equation (6) into the left-hand side and using the relation $pv_m = RT_m$ to rewrite the right-hand side, equation (34) is transformed as

$$\frac{4g}{d\gamma_m u_m^2} S_{ao} = \frac{1}{T_m}\frac{dT_m}{dx} - \frac{1}{p}\frac{dp}{dx}. \tag{101}$$

Second, the equation of motion (3) is expressed, by using equation (4) and neglecting the gravity force, as

$$-\frac{dp}{dx} = \frac{4}{d}(S_{ao} + \tau_w). \tag{102}$$

Thirdly, the energy equation for steady flow:

$$C_p\frac{dT_m}{dx} + \frac{A}{g}u_m\frac{du_m}{dx} = \frac{\pi dq_w}{\frac{\pi}{4}d^2u_m\gamma_m}$$

is transformed. by using equation (6) to rewrite the second term on the left-hand side, as

$$c_p\frac{dT_m}{dx} + \frac{4A}{d\gamma_m}S_{ao} = \frac{4q_w}{d\gamma_m u_m}. \tag{103}$$

Substituting equations (102) and (103) into equation (101) to eliminate dT_m/dx and dp/dx, we obtain

$$S_{ao}\left(\frac{gRT_m}{u_m^2} + \frac{AR}{c_p} - 1\right) = \frac{R}{c_p}\frac{q_w}{u_m} + \tau_w$$

where $AR/c_p = (\kappa - 1)/\kappa$, and $M_m = [u_m/\sqrt{(\kappa g R T_m)}]$ is a Mach number. Thus,

$$S_{ao}\left(\frac{1}{\kappa M_m^2} - \frac{1}{\kappa}\right) = \frac{R}{c_p}\frac{q_w}{u_m} + \tau_w.$$

Whence we obtain

$$\frac{S_{ao}}{\tau_w} = \frac{\kappa M_m^2}{1 - M_m^2}\left(\frac{R}{c_p}\frac{q_w}{u_m\tau_w} + 1\right)$$
$$= \frac{1}{1 - M_m^2}\left(\frac{u_m}{gc_pT_m}\frac{q_w}{\tau_w} + \kappa M_m^2\right). \tag{104}$$

By comparing this with equation (39), we obtain a relation:

$$\frac{S_{ao}}{\tau_w} = \frac{1}{1 - M_m^2}\left\{\left(\frac{S_{ao}}{\tau_w}\right)_{M=0} + \kappa M_m^2\right\} \tag{105}$$

where $(S_{ao}/\tau_w)_{M=0}$ represents the value of S_{ao}/τ_w that is calculated by assuming equation (39) for low speed flow. By the way, when $q_w = 0$, we have the case of Fanno flow, that is, the adiabatic flow with friction [43].

EFFETS D'ARCHIMEDE ET D'ACCELERATION DUS À LA DILATATION THERMIQUE EN CONVECTION TURBULENTE FORCÉE DANS DES TUBES CIRCULAIRES VERTICAUX—CRITÈRES DES EFFETS, PROFILS DE VITESSE ET DE TEMPÉRATURE ET TRANSITION INVERSE DEPUIS L'ÉCOULEMENT TURBULENT À L'ÉCOULEMENT LAMINAIRE

Résumé—On considère dans cet article le transfert de chaleur et de quantité de mouvement par turbulence pour un fluide forcé à travers un tube vertical. Tout d'abord, les auteurs étudient une distribution de contrainte tangentielle dans un tube en considérant la force d'Archimède ainsi que la force d'intertie dues

à l'accélération. Il est prouvé que les effets de ces deux forces sont semblables et résultent d'une diminution rapide de la contrainte tangentielle près de la paroi. La façon dont le profil de vitesse dépend du gradient de contrainte tangentielle à la paroi a permis aux auteurs de déduire les critères pour les effets d'Archimède et d'accélération. Ils proposent enfin un critère basé sur la théorie précédente de la transition inverse de l'écoulement turbulent à l'écoulement laminaire.

AUFTRIEBS- UND BESCHLEUNIGUNGSEFFEKTE AUFGRUND VON THERMISCHER EXPANSION BEI ERZWUNGENER TURBULENTER KONVEKTION IN SENKRECHTEN KREISFÖRMIGEN ROHREN. KRITERIEN DER EFFEKTE, GESCHWINDIGKEITS- UND TEMPERATUR-PROFILE, UND RÜCKLÄUFIGER ÜBERGANG VON TURBULENTER ZU LAMINARER STRÖMUNG

Zusammenfassung—Es werden turbulente Wärme- und Impulsübertragung für ein Fluid, das durch ein vertikales Rohr strömt, behandelt. Erstens wird die Scherspannungsverteilung in einem Rohre untersucht bei Berücksichtigung von Auftriebs- und Trägheitskräften. Es wird gezeigt, dass die Effekte der beiden Kräfte sehr ähnlich in Erscheinung treten und daher ein sehr rascher Abfall der Scherspannung nahe der Wand auftritt. Durch Berücksichtigung der Abhängigkeit des Geschwindigkeitsprofils vom Scherspannungsgradienten an der Wand leiten die Autoren Kriterien für die Einflüsse von Auftrieb und Beschleunigung her. Zweitens wird eine Näherungstheorie vorgeschlagen, für die Berechnung von Geschwindigkeits- und Temperaturprofilen unter Einfluss von Auftrieb und Beschleunigung, unter der Annahme, dass die turbulente Grenzschichtströmung durch Überlagerung von lokal entwickelten Strömungen gebildet wird. Drittens wird aufgrund der vorgenannten Theorie ein Kriterium für den rückläufigen Übergang von turbulenter zu laminarer Strömung vorgeschlagen.

ВЛИЯНИЕ ПОДЪЁМНОЙ СИЛЫ И УСКОРЕНИЯ ЗА СЧЁТ ТЕПЛОВОГО РАСШИРЕНИЯ НА ВЫНУЖДЕННУЮ ТУРБУЛЕНТНУЮ КОНВЕКЦИЮ В ВЕРТИКАЛЬНЫХ ТРУБАХ КРУГЛОГО СЕЧЕНИЯ

Критерии оценки эффэктов подъемной силы и ускорения, профилей скорости и температуры и обратного перехода от турбулентного течения к ламинарному

Аннотация—В статье рассматривается турбулентный перенос тепла и импульса для жидкости, прокачиваемой через вертикальную трубу. Во-первых, исследуется распределение сдвигового напряжения в трубе с учётом подъёмной силы, а также силы инерции за счёт ускорения. Доказано, что эффект дейсивия обоих сил весьма схож и приводит к очены быстрому уменьшению сдвигового напряжения вблизи стенки. С помощью зависимости профиля скорости от градиента сдвигового напряжения на стенке выводятся критерии основных эффектов действия подъёмной силы и ускорения. Во-вторых, в предположении, что турбулентный пограничный слой образуется наложением локально развитых слоев, предлагается приближенная теория расчета профилей скорости и температуры в случае больших эффектов подъемной силы и ускорения. В-третьих, на основе вышеуказанной теории предложен критерий обратного перехода от турбулентного течения к ламинарному.